

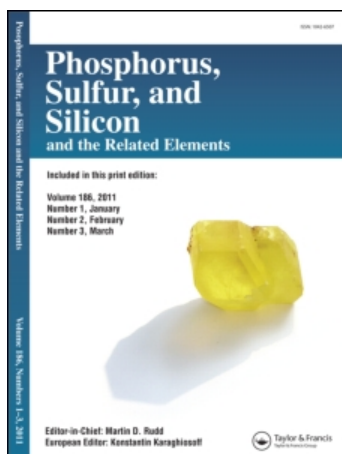
This article was downloaded by:

On: 28 January 2011

Access details: *Access Details: Free Access*

Publisher *Taylor & Francis*

Informa Ltd Registered in England and Wales Registered Number: 1072954 Registered office: Mortimer House, 37-41 Mortimer Street, London W1T 3JH, UK



## Phosphorus, Sulfur, and Silicon and the Related Elements

Publication details, including instructions for authors and subscription information:

<http://www.informaworld.com/smpp/title~content=t713618290>

## Proton NMR Imaging in Dental Systems

Olivier Beuf; Michele Lissac; Andre Briguet

**To cite this Article** Beuf, Olivier , Lissac, Michele and Briguet, Andre(1999) 'Proton NMR Imaging in Dental Systems', Phosphorus, Sulfur, and Silicon and the Related Elements, 144: 1, 425 — 428

**To link to this Article:** DOI: 10.1080/10426509908546272

**URL:** <http://dx.doi.org/10.1080/10426509908546272>

PLEASE SCROLL DOWN FOR ARTICLE

Full terms and conditions of use: <http://www.informaworld.com/terms-and-conditions-of-access.pdf>

This article may be used for research, teaching and private study purposes. Any substantial or systematic reproduction, re-distribution, re-selling, loan or sub-licensing, systematic supply or distribution in any form to anyone is expressly forbidden.

The publisher does not give any warranty express or implied or make any representation that the contents will be complete or accurate or up to date. The accuracy of any instructions, formulae and drug doses should be independently verified with primary sources. The publisher shall not be liable for any loss, actions, claims, proceedings, demand or costs or damages whatsoever or howsoever caused arising directly or indirectly in connection with or arising out of the use of this material.

## Proton NMR Imaging in Dental Systems

OLIVIER BEUF<sup>a</sup>, MICHELE LISSAC<sup>b</sup> and ANDRE BRIGUET<sup>a</sup>

<sup>a</sup>Laboratoire de RMN, CPE Lyon, 43, Boulevard du 11 novembre 1918,  
69622 Villeurbanne Cedex, France and <sup>b</sup>Faculté d'Odontologie, rue Guillaume  
Paradin, 69372 Lyon Cedex 08, France

NMR methods for the analysis of the interface between tissues and prosthetic biomaterials are presented and applied to dental materials. The generation of susceptibility artifacts is explained and their correction is achieved. Results for *in vitro* and *in vivo* proton microscopic imaging of teeth and of the jaw area in mammals are given. Further applications of artifact compensation are indicated for imaging the mineral part of bone samples *in vitro*.

**Keywords:** MRI; susceptibility artifacts; dental systems; bones imaging; biomaterials

### INTRODUCTION

Recent developments of mini-and micro-imaging techniques permit one to obtain highly spatially resolved images (resolution less than 50  $\mu\text{m}$  per pixel) and to study hard tissues (bones, cartilages, tendons) as well as soft tissues. The present work investigates proton dental imaging, an unusual field for magnetic resonance imaging. The problem of artifacts between dental prosthetic biomaterials and living tissues is presented with the aim of determining susceptibility values and compensating for the image artifacts produced. Then mammalian dental images are demonstrated and the possibility of performing high resolution maps of the mineral content of bones is discussed.

### SUSCEPTIBILITY ARTIFACTS AND THEIR CORRECTION

Routine observations of the dental system using MRI highlight the disastrous effect of prosthetic materials upon head imaging. Due to their strong magnetic susceptibility, some materials distort the static magnetic field and may create huge image distortions. In such conditions, reliable observation of the brain area cannot be performed. Given the variety of materials, it is interesting to know the total range of their magnetic

susceptibility values. Under certain conditions, susceptibility measurements can be made directly with MRI, since the size and shape of the induced distortions can be predicted from straightforward magnetostatic calculations<sup>[1]</sup>. This works well when the absolute value of the susceptibility to be determined is no larger than 1000 ppm (part per million), and the condition is fulfilled for a large variety of materials as indicated in Table I, where results are expressed in ppm.

TABLE I : Some magnetic susceptibility values of commonly employed prosthetic materials, measured by NMR imaging techniques.

Non precious samples	$\chi$ (ppm) obtained by PR	$\chi$ (ppm) obtained by 2DFT	$\chi$ (ppm) by <sup>[1]</sup> R. Davis method
T40 (99.8% Ti)	169 ± 17	180 ± 23	181 ± 5
TA6V (89% Ti, 6% Al, 4.4% V)	173 ± 17	195 ± 24	189 ± 6
Cr-Co (89% Ti, 6% Al, 4.4% V)	856 ± 67	989 ± 94	920 ± 10

The results presented above have been obtained from distance measurements<sup>[1]</sup> on images of well calibrated samples placed in distilled water ( $\chi = -9,05 \times 10^{-6}$  ppm). Using a cylindrical model with its axis oriented perpendicularly to the static field, it is possible to correlate the size of the susceptibility artifacts at the interface between water and solid to its susceptibility value. The relative sign of the susceptibility with respect to the medium surrounding the sample is a valuable supplementary piece of information that can be obtained. The choice of the imaging strategy (two dimensional Fourier Transform, 2DFT or Projection Reconstruction, PR) may also change the distortion shape, giving the ability to confirm measurement results.

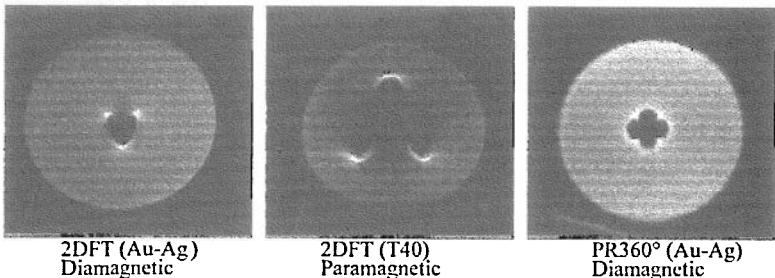


FIGURE 1 Different artifacts observed at 2 Tesla on sample of 8mm diameter.

The influence of the sequence design on the results demonstrates that certain imaging procedures can be expected to be less sensitive to susceptibility effects. In fact it is possible to obtain images free of susceptibility artifacts by using gradient reversal techniques or multiple phase encoding strategies combined with fast imaging modalities. The price to be paid is the length of the raw data acquisition time. Nevertheless this represents the most efficient way to remove image distortions, the same technique being valid for any high field imaging procedure and especially for imaging dental system in the presence of prosthetic materials.

### IN VITRO AND IN VIVO NMR IMAGES OF TEETH

The experiments reported here have been performed in a static field of 2 Tesla with an Oxford 85/310 horizontal magnet associated to a SMIS IVS console. The maximum gradient value employed was about 50 mT/m. For *in vivo* experiments with rats (Male Sprague-Dawley rats of 3 and 12 weeks old) multislice spin echo sequence ( $T_2$  weighted experiments) were employed ( $TE =$  from 19 to 50 ms,  $TR =$  1500 or 3000ms, slice thickness = 700 $\mu$ m).

*In vitro*, the hemi-mandible rat images, obtained with a Helmholtz radiofrequency coil, show three erupted molars (Fig. 2). The molar pulp was observed in homothetic form with the teeth and appears as a hyperintensity signal. The periodontal ligament, the calcified tissues and the pulp of the incisor are also clearly seen<sup>[2]</sup>.

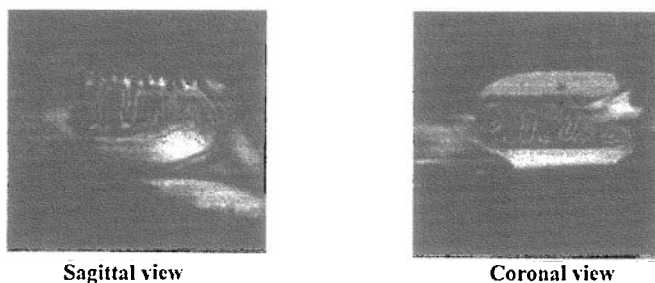


FIGURE 2 In vitro imaging of the jaw of a 12 weeks old rat (field of view 15x15 mm<sup>2</sup>).

*In vivo* images of a young rat were obtained using a half bird cage coil and the slices shown in Fig. 3 correspond to molar roots. One can distinguish the first molars anchored by 4 roots, from left to right.

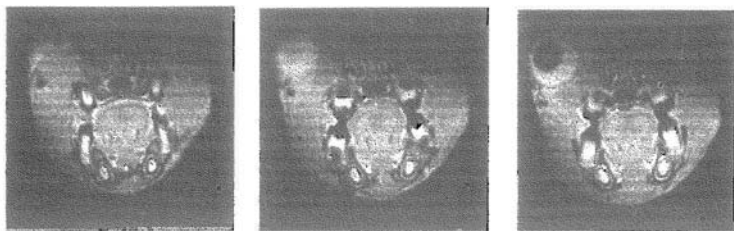


FIGURE 3 Transverse slices of a rat head showing molar and incisors structures.

### OTHER POSSIBILITIES : IMAGING OF BONE MINERAL CONTENT

Two kinds of measurements can be performed : analysis of the bone marrow signal decay [3,4] and microimaging of the trabecular structure [5,6]. A modified sequence, where radiofrequency excitation is achieved by non spatially selective pulse to obtain 3D spin-echo images,[7] was used. The spatial resolution obtained is isotropic ( $60 \times 60 \times 60 \mu\text{m}^3$ ) and the internal bone architecture is illustrated here by a comparison between the calcified volume of a one-legged 91 year-old man and that of a 76 year-old woman. (Fig. 4, left and right respectively).

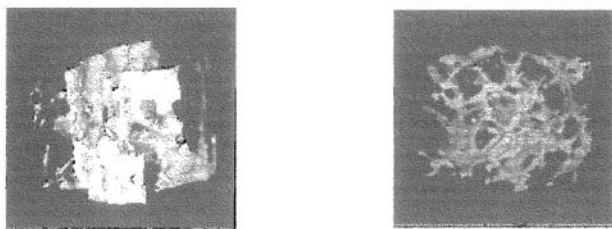


FIGURE 4 High resolution representation of the bone mineral content using magnetic resonance (size of the represented samples :  $3 \times 3 \times 3 \text{ mm}^3$ ).

### References

- [1] O. Beuf, A. Briguet, M. Lissac and R. Davis, *J Magn. Reson B*, **112**, 111 (1996)
- [2] O. Beuf, A. Briguet and M. Lissac, *Oral Surg Oral Med Oral Pathol Oral Radiol Endod*, **84**, n°5, 582 (1997)
- [3] F. Majumdar and H.K. Genant, *Osteoporosis-Int.*, **5**(2), 79 (1995)
- [4] J.A. Hopkins and F. W. Wehrli, *Magn.Reson.Med.*, **37**, 494 (1997)
- [5] F.W. Wehrli, J.C. Ford, H.W. Chung, S.L. Wehrli, J.L. Williams, M.J. Grimm, S.D. Kugel, *Calcif. Tissue Int.*, **53**, S162 (1993)
- [6] H. Jara, F.W. Wehrli and J.C. Ford, *Magn.Reson.Med.*, **29**, 528 (1993)
- [7] J. Ma, F. Wehrli; H.K. Song, *Magn.Reson.Med.* **35**, 903-910 (1996)